Received: 13 March 2023 | Revised: 28 April 2023 | Accepted: 4 May 2023

https://doi.org/10.1016/j.rpth.2023.100184

ORIGINAL RESEARCH

Regulation of megakaryo/thrombopoiesis by endosomal toll-like receptor 7 and 8 activation of CD34$^+$ cells in a viral infection model

Camila Sofía Rodríguez BSc[1] | Nancy Charó PhD[1] | Silvio Tatti MD[2] | Ricardo Martín Gómez MD, PhD[3] | Lina Paola D'Atri PhD[1] | Mirta Schattner PhD[1]

[1]Laboratory of Experimental Thrombosis and Immunobiology of Inflammation, IMEX-CONICET-National Academy of Medicine, Buenos Aires, Argentina

[2]Clinical Hospital, Buenos Aires, Argentina

[3]Laboratory of Animal Viruses, Institute of Biotechnology and Molecular Biology, UNLP-CONICET, La Plata, Argentina

Correspondence
Mirta Schattner and Lina Paola D'Atri, Laboratory of Experimental Thrombosis and Immunobiology of Inflammation, IMEX-CONICET-National Academy of Medicine, Pacheco de Melo 3081, Buenos Aires (1425), Argentina.
Email: lpdatri@hotmail.com and mschattner@hotmail.com

Handling Editor: Prof Yotis Senis

Abstract

Background: CD34$^+$ cells, megakaryocytes (MKs), and platelets express toll-like receptors (TLRs) that enable these cells to amplify the host innate immune response. However, the role of TLR7/TLR8 activation in megakaryopoiesis has not yet been investigated.

Objectives: We evaluated the effect of coxsackievirus B3 (CVB3) and synthetic TLR7/TLR8 agonists on the development of human MKs and production of platelets.

Methods: CD34$^+$ cells from human umbilical cord were inoculated with CVB3 or stimulated with synthetic TLR7/TLR8 agonists and then cultured in the presence of thrombopoietin.

Results: CD34$^+$ cells, MK progenitor cells, and mature MKs expressed TLR7 and TLR8, and exposure to CVB3 resulted in productive infection, as determined by the presence of viral infectious particles in culture supernatants. Cell expansion, differentiation into MKs, MK maturation, and platelet biogenesis were significantly reduced in CD34$^+$-infected cultures. The reduction in MK growth was not due to an alteration in cellular proliferation but was accompanied by an increase in cellular apoptosis and pyroptosis. Impairment of MK generation and maturation of viable cells were also associated with decreased expression of transcription factors involved in these processes. These effects were completely abrogated by TLR7 but not TLR8 antagonists and mimicked by TLR7 but not TLR8 agonists. CVB3 infection of CD34$^+$ cells increased the immunophenotype of MKs characterized as CD148$^+$/CD48$^+$ or CD41$^+$/CD53$^+$ cells.

Conclusion: These data suggest a novel role of TLR7 in megakaryo/thrombopoiesis that may contribute to a better understanding of the molecular basis underlying thrombocytopenia and the immunologic role of MKs in viral infection processes.

Lina Paola D'Atri and Mirta Schattner contributed equally to this study.

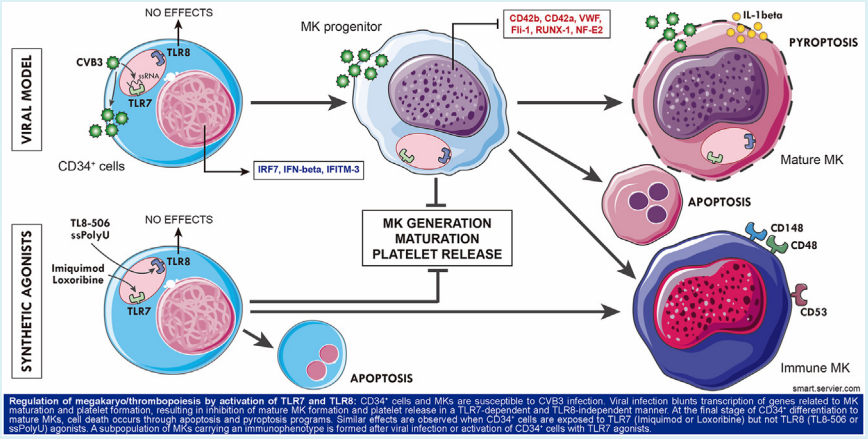

KEYWORDS
megakaryocytes, platelets, RNA viruses, toll-like receptor 7, toll-like receptor 8

Essentials

- The role of receptors that sense viruses in megakaryocyte and platelet production is unknown.
- Human stem cells were used to study platelet biogenesis in a viral infection model.
- Virus recognition by toll-like receptor 7 (TLR7) impairs megakaryocyte and platelet development.
- Viral infection and TLR7 activation increase megakaryocytes with immune properties.

1 | INTRODUCTION

Pathogen recognition is mediated by pattern recognition receptors (PRRs), including toll-like receptors (TLRs). TLRs are transmembrane receptors found on both the plasma membrane and endosomal vesicles. Upon ligation, TLRs trigger the expression of proinflammatory cytokines, chemokines, and costimulatory and adhesion molecules, resulting in activation of the adaptive immune system and initiation of inflammatory responses [1]. Although not immune cells, platelets express all members of the TLR family, and their activation has been shown to play a role in the amplification of the host's innate immune response against bacterial and viral infections [2–4].

However, in contrast to several studies on murine cells or cell lines, the expression of TLRs in human hematopoietic stem and progenitor cells (HSPCs) or megakaryocytes (MKs) and their potential regulation of megakaryo/thrombopoiesis are still poorly characterized. In this sense, TLR2 and TLR4 were identified in human bone marrow $CD34^+$ cells, and it was found that they are upregulated in apoptotic $CD34^+$ cells from patients with myelodysplastic syndromes, possibly contributing to cytopenia seen in these patients [5–7]. We showed that TLR2 and TLR4 activation in $CD34^+$ cells increased thrombopoietin (TPO)-induced human $CD34^+$ cell proliferation, MK number, maturity, and proplatelet and platelet production through activation of the PI3K and NF-κB pathways and interleukin (IL)-6 generation [8]. These data suggest that activation of TLR2 and TLR4 in human $CD34^+$ cells and MKs in the presence of TPO contributes to ensuring platelet delivery during infection. Indeed, reactive thrombocytosis is generally associated with bacterial infections [9].

Thrombocytopenia is frequently observed in acute viral infections, and low platelet counts are a hallmark of poor prognosis in many infectious diseases. The underlying mechanisms of virus-induced thrombocytopenia are not clearly understood and may be related to a functional alteration in circulating platelets and/or bone marrow stem cells and MKs. A low platelet count could be the result of a direct effect of viruses or the combined effect of cytokines and the host immune response on platelet, HSPC, and MK functionality [10,11]. Nevertheless, reduced megakaryopoiesis due to lower TPO production in the liver during infection has also been suggested [12].

Viral genomes are mainly recognized by endosomal TLRs, such as TLR3, TLR7, and TLR8, which sense double-stranded RNA (dsRNA) and single-stranded RNA (ssRNA), respectively. We have shown that human cells from the megakaryocytic lineage express functional TLR3. Stimulation of MKs with 2 synthetic agonists of TLR3, poly(I:C) and poly(A:U), decreased platelet production *in vitro* and triggered the release of interferon (IFN)-β through the PI3K-Akt and NF-κB signaling pathways, suggesting a possible role of TLR3 activation in the downregulation of platelet production that occurs during some viral infections [13]. Thrombocytopenia has also been reported in infections mediated by ssRNA viruses, such as HIV [14], coxsackie [15,16], and influenza [17], and in patients infected with severe coronavirus diseases, including severe SARS-CoV2 infection [18,19]. Platelets can engulf influenza A virus, resulting in the formation of C3 complement, which causes release and aggregation of neutrophil DNA

as a function of platelet TLR7 [20]. Moreover, it has been shown that platelets can also internalize SARS-CoV-2, leading to platelet apoptosis [21]. Interestingly, although these studies showed that influenza or SARS-CoV-2 platelet interactions lead to platelet activation, which may be responsible for thrombotic events, platelet consumption during these episodes may also explain the decrease in platelet count. Of note, using a mouse model, Zhang et al. [22] demonstrated that upregulation or downregulation of the TLR7 pathway leads to inhibition of or increase in platelet count, respectively. Another possibility for thrombocytopenia in ssRNA viral infections that has not yet been investigated could be the activation of TLR7/TLR8 in MKs or stem cells in the bone marrow. To gain further insight into the role of these endosomal receptors in the regulation of megakaryo/thrombopoiesis, we aimed to analyze the effect of infection of HSPCs ($CD34^+$ cells) and MKs with coxsackievirus B3 (CVB3) used as an ssRNA virus model and with synthetic agonists of TLR7 and TLR8.

2 | METHODS

2.1 | Reagents

StemSpan serum-free medium was purchased from StemCell Technologies. TPO and CD34 purification kit were purchased from Miltenyi Biotec. Click-iT Plus EdU Alexa Fluor-488, Alexa Fluor-488 anti-mouse IgG, Alexa Fluor-647 anti-mouse IgG1, and Alexa Fluor-647 anti-mouse IgG2a, and 4',6-diamidino-2-phenylindole, dilactate, were purchased from Invitrogen. Anti-CD53-fluorescein isothiocyanate (FITC), anti-CD148-PE, anti-CD48-APC, mouse anti-TLR8 antibody (Ab) (clone S16018A), annexin-V-FITC, Zombie Violet Fixable Viability Dye, and enzyme-linked immunosorbent assay (ELISA) MAX Deluxe Set Human IL-1β were purchased from Biolegend. Cleaved caspase-3 (Asp175) was purchased from Cell Signaling Technology. Anti-CD34-FITC, anti-CD61-FITC, anti-CD42b-FITC, anti-CD42a-FITC, anti-CD41-PE, mouse anti-actin (Ab-5), horseradish peroxidase (HRP)–labeled goat anti-rabbit and HRP goat anti-mouse were purchased from BD Biosciences. Von Willebrand factor (VWF) Ab was purchased from Inmunotech and mouse anti-TLR7 Ab (clone 4G6) from NOVUS Biologicals. Mouse anti-TLR7 (clone 4F4), mouse anti-TLR8 (clone D-8), rabbit anti-IL-1β, and rabbit anti-caspase-1 were purchased from Santa Cruz Biotechnology. Rabbit anti-gasderminD (GSDMD) was purchased from Proteintech. VeriKine-HS (High Sensitivity) Human IFN-β TCM ELISA kit was purchased from PBL Assay Science. Bio-Zol was purchased from PB-L Productos Bio-Lógicos. SsoAdvanced Universal SYBR Green Supermix and iScript complementary DNA synthesis kits were purchased from Bio-Rad Laboratories. TLR7/8 (ODN2087) and TLR7 (ODN20958) antagonists were purchased from Miltenyi Biotec. Imiquimod (R837), loxoribine, ssPolyU, TL8-506, and the TLR8 inhibitor (CU-CPT9a) were purchased from Invivogen. Inhibitors of the inflammasome components were purchased from Cayman Chemical.

2.2 | Isolation of $CD34^+$ cells

$CD34^+$ cells were isolated from human umbilical cord blood that was collected during normal full-term deliveries as previously described [8]. $CD34^+$ cells were purified from blood mononuclear cells using a magnetic cell sorting system in accordance with the manufacturer's recommendations. Purity of the cell suspension ranged between 95% and 99%, and viability was >95%.

2.3 | Vero cells

Vero cells were obtained from the American Type Culture Collection and maintained as monolayers in RPMI-1640 medium (Gibco), supplemented with 10% heat-inactivated fetal bovine serum (Gibco) and antibiotics (100-U/mL penicillin and 100-μg/mL streptomycin), and incubated at 37 °C at 5% carbon dioxide in a humidified incubator.

2.4 | Virus culture

CVB3 and yellow fever virus (YFV) were amplified on 80% confluent Vero cells at a multiplicity of infection (MOI) of 1. Supernatant was collected 20 hours or 7 days later, respectively, centrifuged, and stored at −80 °C. The virus stocks were quantified using the standard plaque assay in Vero cells. Inactivation of CVB3 or YFV was performed by exposing the virus stock to UV light, as described previously [23], and UV-irradiated CVB3 (CVB3 UV) or UV-irradiated YFV (YFV UV) were used as a negative control (mock). UV inactivation was confirmed using the plaque assay.

2.5 | Cell infection

Cells were infected with CVB3, YFV, or CVB3 UV or YFV UV for 1 hour in a polypropylene tube or plate (adherent cells) at 37 °C, followed by 3 washes with phosphate-buffered saline.

After washing, virus- or mock-infected $CD34^+$ cells were cultured in StemSpan medium supplemented with 50-ng/mL TPO and antibiotics at 37 °C in a humidified atmosphere with 5% carbon dioxide. Fresh TPO (25 ng/mL) was added on day 7.

2.6 | Flow cytometry (FC) studies

To evaluate MK differentiation and maturation, cells were double stained with anti-CD41-PE and anti-CD42b-FITC. The intracellular expression of TLR7 and TLR8 was determined by first labeling cells with Zombie Violet viability dye to exclude dead cells from the analysis and then fixing and permeabilizing them with BD Cytofix/Cytoperm. The cells were then incubated with mouse anti-TLR7 or anti-TLR8 Abs, followed by Alexa Fluor-647 anti-mouse IgG1 or Alexa Fluor-647 anti-mouse IgG2a plus anti-CD34-FITC, anti-CD61-FITC, or

anti-CD42b-FITC after 0, 6, and 12 days of culture to identify TLRs in $CD34^+$ cells, MK progenitors, and mature MKs.

Intracellular VWF was evaluated by fixing and permeabilizing cells with BD Cytofix/Cytoperm and labeling with anti-VWF followed by Alexa Fluor-488 anti-mouse. Inflammatory MKs were identified by triple or double staining of viable cells with anti-CD42b-FITC/CD148-PE/CD48-APC or CD41-PE/CD53-FITC. The intracellular expression of TLR7 and TLR8 on viable immune MKs ($CD148^+/CD48^+$) was determined by incubating cells with anti-TLR7 or anti-TLR8 Abs followed by anti-mouse Alexa Fluor-488.

The number of platelets was determined after 17 days of culture by staining cells with anti-CD61-FITC Ab or an irrelevant isotype. Culture-derived platelets were counted as $CD61^+$ events with the same scatter properties as human peripheral blood platelets [24].

The percentage of positive cells and the median fluorescence intensity were analyzed using Sysmex-Partec CyFlow Space and FlowJo 10.0.7 software.

2.7 | Immunofluorescence assays

Cells were cytospun, fixed (4% paraformaldehyde), permeabilized (0.1% Triton X-100), and blocked (5% equine serum). To identify CVB3-infected MKs, cells were incubated with anti-dsRNA monoclonal Ab J2 (SCICONS) followed by anti-mouse-Alexa Fluor-488 and CD41-PE. The percentage of $J2^+$ cells in the MK population was calculated using the ImageJ program on at least 200 cells.

To identify the expression of TLRs in immune MKs, cells were incubated with anti-TLR7 (clone 4G6) or anti-TLR8 (clone S16018A) followed by anti-mouse-Alexa Fluor-488, CD148-PE, and CD48-APC.

Infected immune MKs were detected by incubating cells with J2, CD148-PE, and CD48-APC. Cell nuclei were stained with 4',6-diamidino-2-phenylindole and mounted with PolyMount.

2.8 | Determination of apoptosis, viability, and proliferation of cells

Cells were labeled with a mixture of acridine orange and ethidium bromide (100 μg/mL) to determine the percentage of cells that had undergone apoptosis or necrosis [25]. Coverglass preparations were counted using a fluorescence microscope, with a minimum of 200 cells scored from each sample. Cell viability was determined on day 12 of culture by double staining cells with Zombie Violet and Annexin-V-FITC and analyzed using FC. For the proliferation assay, cells were incubated with Zombie Violet, the ethynyl-2′-deoxyuridine detection system, and then analyzed using FC.

2.9 | Analysis of ploidy

The ploidy of MKs was evaluated on day 14 of culture by fixing cells in 70% ice-cold ethanol and then washing and labeling with anti-CD61-FITC monoclonal Ab and propidium iodide (0.5 μg/mL) in the presence of RNAse-A (400 μg/mL) at 37 °C. After 30 minutes of incubation, the cells were immediately analyzed using FC.

2.10 | Analysis of caspase-3 activation

Cells were fixed with 4% paraformaldehyde and permeabilized in 90% ice-cold methanol for 30 minutes. After labeling with a polyclonal rabbit Ab for the activated form of caspase-3, cells were washed, incubated with anti-rabbit Alexa Fluor-488, and analyzed using FC.

2.11 | Quantitative polymerase chain reaction

RNA was isolated with Bio-Zol. Reverse transcription was performed using 150 ng of RNA by employing the iScript complementary DNA synthesis kit. Real-time polymerase chain reactions were assessed by employing the SsoAdvanced universal SYBR Green mix and CFX-Connect equipment (Bio-Rad). The primers used in this study are listed in Supplementary Table S1. The reaction was normalized to the expression levels of the housekeeping gene, and the specificity of the amplified products was checked through analysis of dissociation curves. To generate heat maps, qCT values obtained using the $2\Delta Ct$ method were normalized to reference values (CVB3 UV). The numbers inside the colored squares are the mean value from each group in a given condition.

2.12 | Measurement of IL-1β and IFN-β levels

IL-1β and IFN-β levels were determined in the supernatants of 24-hour, 7-day, and 12-day cultured $CD34^+$ cells using commercial ELISA kits.

2.13 | Western blotting

CVB3-UV– or CVB3-infected MKs were lysed with a lysis buffer (60mM de tris/hydrochloric acid/1% sodium dodecyl sulfate; pH, 6.8) in the presence of a cocktail of protease inhibitors (Sigma). The lysates were electrophoresed and transferred to a polyvinylidene fluoride membrane. After blocking, the membranes were incubated with anti-IL-1β, anti-caspase-1, or anti-GSDMD followed by an HRP-conjugated secondary Ab. Each membrane was reprobed with an Ab against actin, and proteins bands were visualized using enhanced chemiluminescence. Immunoblotting results were semiquantitated using the ImageJ software.

2.14 | Statistical analysis

Data are expressed as mean ± SEM. The Shapiro-Wilk test was used to define state normality and equal variance. Significant differences

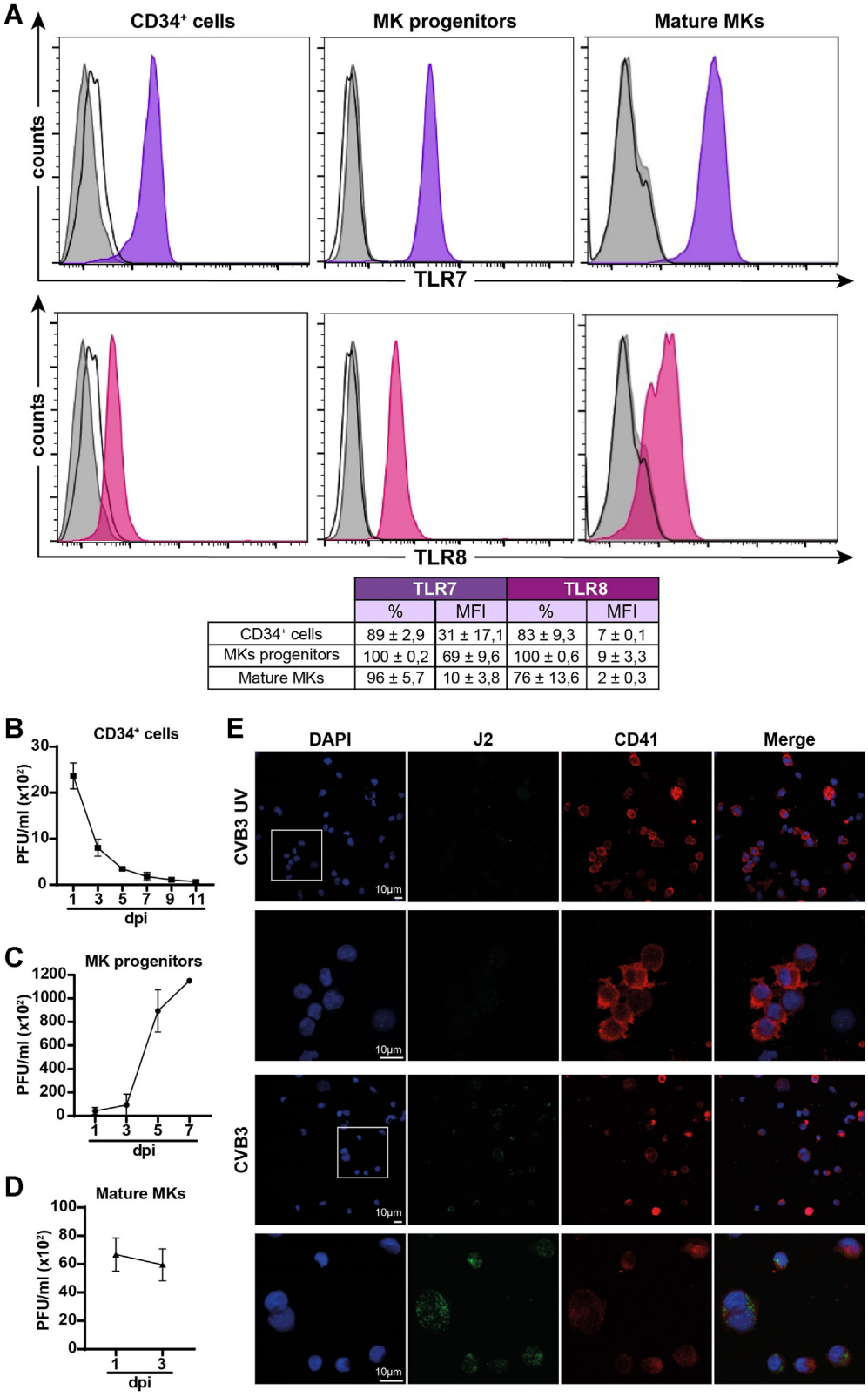

	TLR7		TLR8	
	%	MFI	%	MFI
CD34⁺ cells	89 ± 2,9	31 ± 17,1	83 ± 9,3	7 ± 0,1
MKs progenitors	100 ± 0,2	69 ± 9,6	100 ± 0,6	9 ± 3,3
Mature MKs	96 ± 5,7	10 ± 3,8	76 ± 13,6	2 ± 0,3

FIGURE 1 Human CD34$^+$ cells, megakaryocyte (MK) progenitors, and mature MKs express Toll-like receptor (TLR)7 and TLR8 and are susceptible to coxsackievirus B3 (CVB3) infection. (A) Intracellular TLR7 and TLR8 expression in CD34$^+$ cells, MK progenitors (CD41$^+$/CD42b$^-$), and mature MKs (CD41$^+$/CD42b$^+$). Black lines represent unstained cells, and gray histograms represent fluorescence minus one for each receptor as a negative control (n = 3). (B) CD34$^+$ cells, (C) MK progenitors, and (D) mature MKs were infected with CVB3 (multiplicity of infection, 1), and plaque-forming units in supernatants were quantitated on different days after infection using the infectivity titration assay in Vero cells (n = 3). (E) CD34$^+$ cells were exposed to UV-irradiated CVB3 or CVB3 (multiplicity of infection, 1), and viral presence was detected at

were determined using 1-way or 2-way analysis of variance followed by the multiple-comparison Bonferroni test. Two-tailed paired Student's *t*-test was used to compare 2 groups. Statistical significance was set at $P < .05$. The analysis was performed using GraphPad Prism software, version 9.0.2.

3 | RESULTS

3.1 | CVB3 infects and replicates in CD34$^+$ cells and MKs

First, we evaluated the expression and regulation of TLR7 and TLR8 on CD34$^+$ cells; cells from day 6 or 12 of culture composed mainly of megakaryocytic progenitors (CD41$^+$/CD42b$^-$) and mature MKs (CD41$^+$/CD42b$^+$), respectively. As shown in Figure 1A, all cells examined expressed both receptors. Similar results were observed when cells were labeled with Abs with 2 different clones (see Methods, data not shown). To further confirm the specificity of the Abs used, we also stained peripheral platelets and neutrophils (cells that barely express TLR7) [26,27] and found that platelets express both receptors, albeit TLR8 in a lower percentage. As expected, neutrophils did not express TLR7 but did express TLR8 (Supplementary Figure S1). To determine the susceptibility of CD34$^+$ cells to CVB3 infection, we examined the presence of infectious viral particles in the supernatants of UV-irradiated or virus-infected cells at different time points after infection using supernatants from infected Vero cells as a positive control. Titration assays revealed that infectious viruses were detected more abundantly in the supernatant of CVB3-infected Vero cells during the first 24 hours, as expected (data not shown). In contrast, infectious viruses from CD34$^+$ supernatants peaked at 24 hours after infection and slowly decreased until they had almost disappeared by day 11 after infection (Figure 1B). In addition, infectious viruses were also observed in supernatants from megakaryocytic progenitors and mature MKs (Figure 1C, D). Interestingly, megakaryocytic progenitors appeared to be most susceptible to CVB3, which was accompanied by an increase in the expression of coxsackievirus and adenovirus receptor, one of the CVB3 receptors [28] (Supplementary Figure S2). The presence of CVB3 was detected in infected MKs by labeling the cells with an Ab that recognizes dsRNA, and the percentage of infected MKs was 41% ± 5% (Figure 1E).

3.2 | Infection of CD34$^+$ cells with CVB3 triggers apoptosis and pyroptosis

Having demonstrated that CVB3 infects CD34$^+$ cells, we next examined the effect of CVB3 infection on megakaryo/thrombopoiesis using an *in vitro* model with human CD34$^+$ cells stimulated with TPO. Under our culture conditions, TPO stimulation promotes the growth of mature MKs and platelets [23]. However, the exposure of CD34$^+$ cells to CVB3, but not to CVB3 UV, decreased the absolute number of cells in an MOI-dependent manner (Figure 2A), including the numbers of MKs (Figure 2B) and platelets produced in culture (Figure 2C). The formation of MKs and platelets in the CD34$^+$ cultures infected with CVB3 UV was similar to that in the uninfected cells (Supplementary Figure S3). To determine whether the decrease in cell growth was related to impaired cell proliferation, apoptosis, or both, we next analyzed the proliferation rate by measuring 5-ethynyl-2′-deoxyuridine (EdU) incorporation into CD34$^+$ cells after 4 days of TPO stimulation in the absence or presence of infective CVB3. As shown in Figure 2D, there were no differences in the incorporation of the thymidine analog regardless of whether the cells were exposed to CVB3 or CVB3 UV. However, an analysis of changes in nuclear morphology, indicative of programmed cell death, showed that CVB3 triggered a significant increase in the percentage of apoptotic cells, which was detected after 12 days after infection (Figure 2E). Programmed cell death was confirmed by an increase in hypodiploid cells (Figure 2F), phosphatidylserine exposure (Figure 2G), and caspase-3 activation (Figure 2H).

Because cells undergoing pyroptosis exhibit features of apoptosis, such as exposure to phosphatidylserine and condensed chromatin [29], we examined whether inflammasome activation also occurs during viral infection. The IL-1β protein level was measured at 24 hours, 7 days, or 12 days after infection; however, it was detected only at a later time point (Figure 3A). In agreement with these results, Western blotting kinetic studies at 6 and 10 days after infection showed that the expression of cleaved forms of caspase-1, IL-1β, and GSDMD were detected only at 10 days after infection (Figure 3B and Supplementary Figure S4). The activation of inflammasomes in infected cells was confirmed based on a greater decrease in immature forms of caspase-1 and IL-β as well as a corresponding increase in their cleaved forms compared with those in the mock samples (Figure 3B). In addition, the presence of NLRP3, caspase-1/4, and caspase-1 inhibitors prevented a decrease in cell number, cell death, differentiation, and maturation of MKs (Figure 3C–F). Collectively, these data indicate that both apoptosis and pyroptosis were induced by viral infection. Necrosis never exceeded 5% in all cases.

3.3 | CVB3 infection of CD34$^+$ cells impairs the generation of mature MKs

CVB3 infection of CD34$^+$ cells not only significantly reduced cell expansion but also markedly inhibited the differentiation of CD34$^+$ cells into MKs and MK maturation. Figure 4A shows that the

9 days after infection. Representative confocal microscopy images show nuclei (blue), J2 staining of double-stranded RNA (green), and CD41 expression (red). Insets: 3× zoom. Scale bar, 10 μm. DAPI, 4′,6-diamidino-2-phenylindole; MFI, median fluorescence intensity; PFU, plaque-forming unit.

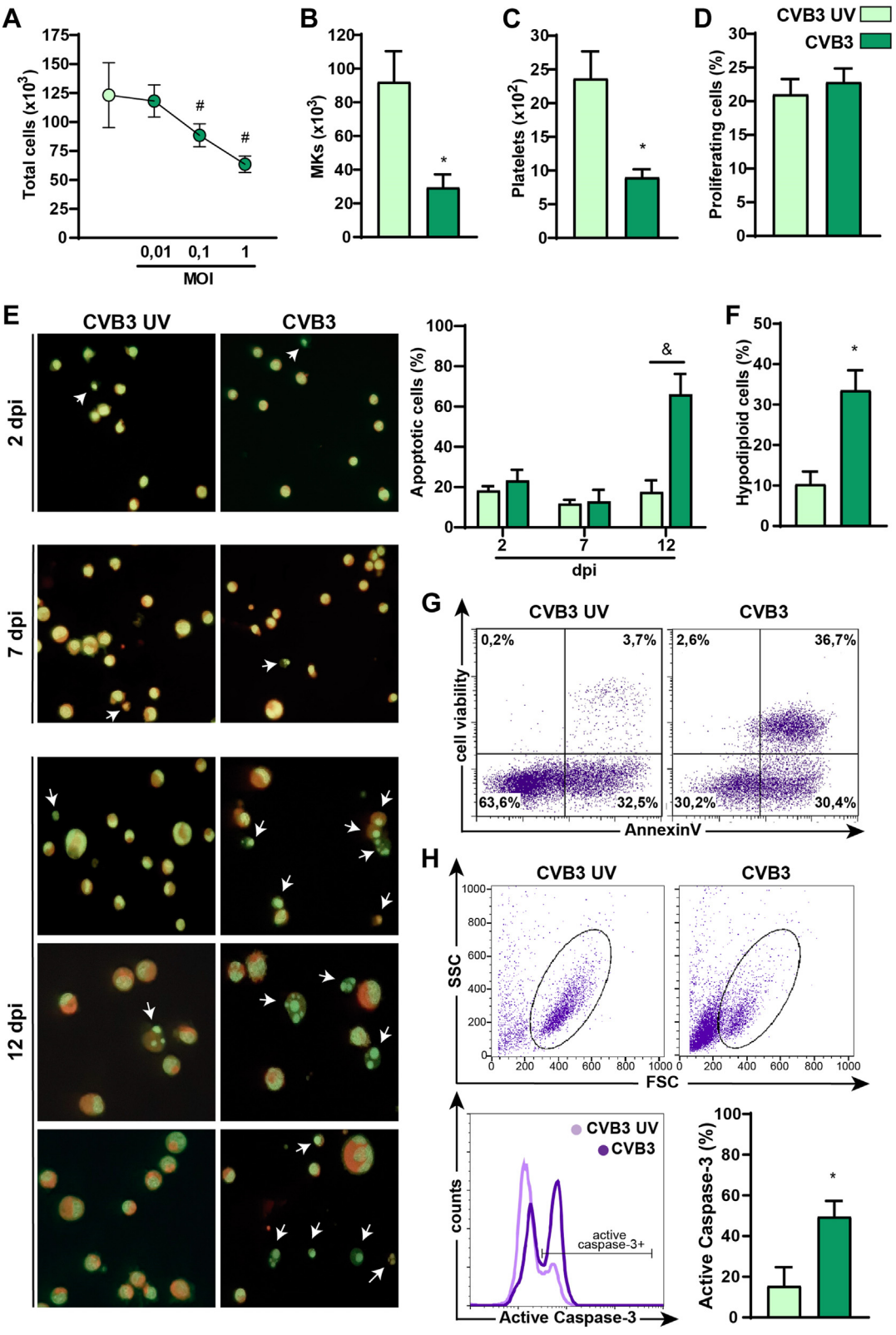

FIGURE 2 Coxsackievirus B3 (CVB3) infection of $CD34^+$ cells inhibits megakaryo/thrombopoiesis. (A) $CD34^+$ cells were exposed to different multiplicities of infection of UV-irradiated CVB3 (CVB3 UV) or CVB3 and then stimulated with thrombopoietin. The number of total cells was determined at 12 days after infection. $CD34^+$ cells were exposed to CVB3 UV or CVB3 at a multiplicity of infection of 1. (B) The number of megakaryocytes was determined according to the number of total cells that expressed CD41. (C) The number of platelets was enumerated using flow cytometry as $CD61^+$ events with the same scatter properties as blood platelets. (D) The percentage of proliferating cells was determined 4 days after infection by measuring 5-ethynyl-2′-deoxyuridine incorporation in the viable subpopulation. (E) Representative

expression of CD41 was significantly reduced in the live cell population compared with that in the mock samples in an MOI-dependent manner. In addition, the expression of glycoprotein (GP)Ib (CD42b), intracellular VWF, and ploidy was significantly lower in CVB3-infected cultures than in CVB3 UV–infected samples (Figure 4B–D).

In platelets, GPIb expression (CD42b) can be regulated by either internalization or shedding [30,31]. To determine the molecular basis of the decreased expression of GPIb because of CVB3 infection, we used several strategies. First, we measured the amount of RNA transcript for *GPIb*; Figure 4E shows that the amount of mRNA increased significantly over time after the addition of TPO and peaked at day 9 in CVB3 UV–treated cells, whereas it was significantly reduced in CVB3-infected cells. We then measured the expression of GPIb in permeabilized cells and found that the intracellular GPIb levels were also lower in CVB3-infected cultures (Figure 4F). Finally, we examined whether the expression of CD42a, the GPIX of the GPIb-V-IX complex, was also inhibited by viral infection and found that the levels of both mRNA and protein were significantly reduced in infected cultures compared with those in the mock samples (Figure 4G, H). Taken together, these data suggest that the reduction in GPIb was not related to protein shedding or internalization but a more general process of inhibition of protein synthesis. Indeed, we also observed that the mRNA levels of transcription factors involved in MK differentiation and maturation as well as platelet biogenesis, such as *RUNX-1*, *FLI1*, and *NF-E2*, were decreased in virus-infected samples (Figure 4H). It is important to note that the RNA studies were performed on cells from day 9 of culture, when there was no significant virus-mediated cell death.

3.4 | CVB3 infection of CD34$^+$ cells triggers the expansion of phenotypically immune MKs

Recently, 2 different groups described MKs with immune phenotypes and functionality in human and mice bone marrow; 1 subset was characterized as cells expressing CD148 and CD48 surface markers, whereas the other expresses CD53. Both subpopulations of immune MKs proliferate upon lipopolysaccharide (LPS) stimulation [32,33]. Surprisingly, we found that CVB3 infection inhibited the generation of mature MKs and platelets but increased *CD148* and *CD48* transcripts on day 11 of CVB3 cultures (Figure 5A), which was correlated with the appearance of a subset of CD148$^+$/CD48$^+$ MKs in the mature MK population (CD42b$^+$ cells) of CVB3-infected but not in CVB3 UV–infected cultures (Figure 5B). Moreover, these immune MKs also expressed both TLR7 and TLR8 and were susceptible to CVB3 infection (Figure 5C, D).

In addition, an increase in *CD53* transcript and the subset of CD53$^+$ MKs was observed in MKs from infected cultures (Figure 5E, F).

We have previously reported that another immunologic property of progenitor cells and mature MKs is that they have antiviral activity because of being both type I IFN producers and responders [34]. Moreover, we have shown that activation of TLR3 selectively impairs platelet production by producing IFN-β [13]. Upon analysis of the IFN pathway in CVB3-infected CD34 cultures, we found that the mRNA levels of *interferon regulatory factor 7* and its downstream associated gene, *IFN-β*, but not *IFN-α* (data not shown), were significantly increased in CVB3-infected samples 24 hours after infection (Figure 5G, H). Recently, interferon-induced transmembrane protein 3, an antiviral protein triggered by IFN-α/β receptor activation that restricts cellular entry of diverse viruses, was shown to be upregulated in platelets and MKs during dengue and influenza viral infections [35], 2 ssRNA viruses. In concordance, the mRNA levels of *interferon-induced transmembrane protein 3* were also upregulated in CVB3-infected cells (Figure 5I). However, we could not detect the IFN-β protein in the supernatants of infected cultures (data not shown). In addition, the incubation of CD34$^+$ cells with a neutralizing Ab against IFN-β failed to abrogate the inhibitory effects on megakaryopoiesis mediated by CVB3 infection (data not shown).

3.5 | TLR7 activation impairs megakaryopoiesis

Having demonstrated that CD34$^+$ cells and MKs express TLR7 and TLR8, we next investigated whether PRRs were involved in the inhibition of megakaryopoiesis mediated by CVB3 infection. We found that ODN2087 and ODN20958, TLR7/8 and TLR7 antagonists, respectively, reversed the CVB3-mediated inhibitory effects on megakaryopoiesis (Figure 6A–E). Interestingly, similar results were obtained when CD34$^+$ cells were infected with YFV, another ssRNA virus of the *Flaviviridae* family (Supplementary Figure S5).

In addition, the stimulation of CD34$^+$ cells with imiquimod (R837), a TLR7 agonist, resulted in a decrease in the number and maturation of MKs and platelet generation (Figure 6F–I). Because imiquimod is also an adenosine receptor antagonist, to confirm TLR7 stimulation, we also used loxoribine, a guanosine analog that does not activate adenosine receptors [36], as a TLR7 agonist. Similar to imiquimod, loxoribine impaired megakaryopoiesis (Figure 6F–I). Both TLR7 agonists also induced cell apoptosis (Figure 6J), although it was detected at an earlier time point (48 hours after stimulation) compared with CVB3 infection and promoted the generation of CD148$^+$/CD48$^+$ and CD53$^+$ MKs (Figure 6K, L). The concentration of both agonists was

images of cell viability evaluated using fluorescence microscopy of cells labeled with a mixture of acridine orange and ethidium bromide. Arrows indicate apoptotic cells. Bar graph quantifying the percentages of apoptosis (to the right of the panel). (F) Percentage of hypodiploid cells, (G) representative dot plots of annexin-V–fluorescein isothiocyanate/Zombie Violet fixable viability dye staining and (H) percentage of active caspase-3 evaluated in the gated population at 12 days after infection. $^{\#}P < .05$ vs CVB3 UV using 1-way analysis of variance, $^{*}P < .05$ vs CVB3 UV using paired *t*-test, $^{\&}P < .05$ vs CVB3 UV on day 12 using 2-way analysis of variance, n = 3-6. MK, megakaryocyte; MOI, multiplicity of infection.

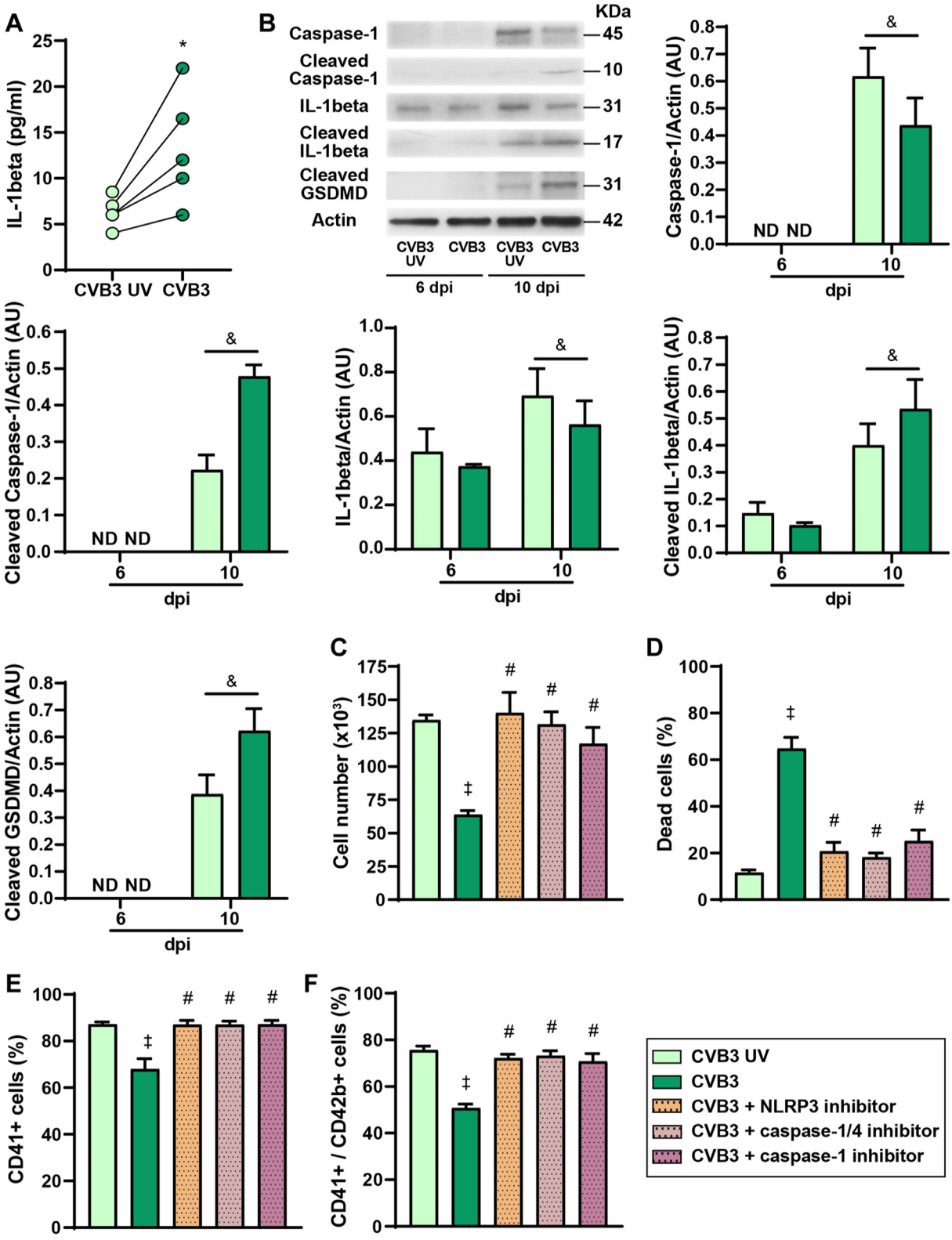

FIGURE 3 Coxsackievirus B3 (CVB3) infection of $CD34^+$ cells induces pyroptosis. $CD34^+$ cells were exposed to UV-irradiated CVB3 (CVB3 UV) or CVB3 (multiplicity of infection, 1). (A) The level of interleukin (IL)-1β was measured in the cell supernatants at 12 days after infection using enzyme-linked immunosorbent assay. (B) Inflammasome activation was evaluated based on the expression of caspase-1, cleaved caspase-1, IL-1β, cleaved IL-1β, and cleaved gasdermin D using Western blotting. (C) The number of cells, (D) percentage of dead cells, (E) $CD41^+$ cells, and (F) $CD41^+/C42b^+$ cells were determined in cultures of thrombopoietin-stimulated $CD34^+$ cells that were exposed to CVB3 UV or CVB3 (multiplicity of infection, 1) and treated or not with MCC950 (NLRP3 inhibitor, 10 μM), VX-765 (caspase-1/4 inhibitor, 50 μM), or Ac-YVAD-CMK (caspase-1 inhibitor, 50 μM) on days 6 and 8 of culture according to the appearance of cleaved forms using Western blotting. $^*P < .05$ vs CVB3 UV using paired *t*-test, $^{\&}P < .05$ vs CVB3 UV on day 10 using 2-way analysis of variance (ANOVA), $^{\ddagger}P < .05$ vs CVB3 UV using 1-way ANOVA, $^{\#}P < .05$ vs CVB3 using 1-way ANOVA, n = 3-6. AU, arbitrary units; ND: not detected; GSDMD, gasderminD.

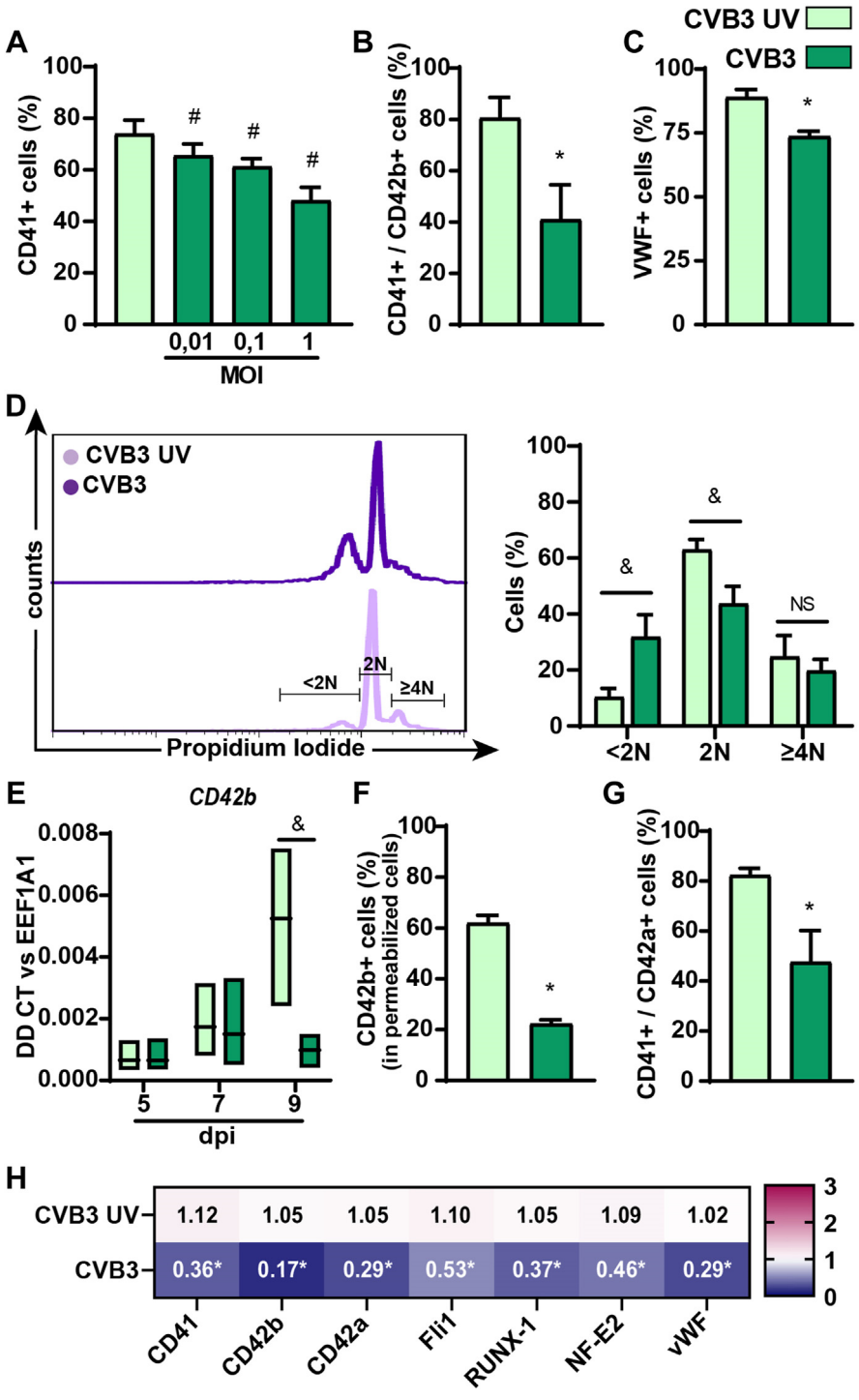

FIGURE 4 Coxsackievirus B3 (CVB3) infection of $CD34^+$ cells inhibits megakaryocyte (MK) differentiation and maturation. (A) $CD34^+$ cells were exposed to different multiplicities of infection of CVB3 or CVB3 UV–irradiated virus, and the percentage of MKs ($CD41^+$ cells) was determined at 12 days after infection using flow cytometry (FC). (B) Cells were infected (multiplicity of infection, 1), and mature MKs ($CD42b^+$ cells gated on $CD41^+$ cells), (C) intracellular von Willebrand factor, and (D) representative histogram and percentages of the ploidy of $CD61^+$ cells (to the right of the panel) were evaluated at 12 to 14 days after infection using FC. (E) The mRNA expression levels of *CD42b* were determined on different days after infection using quantitative polymerase chain reaction and referred to as 2ΔCt. *EEF1A1* was used as the housekeeping gene. (F) Analysis of intracellular $CD42b^+$ and (G) $CD41^+/CD42a^+$ cells using FC. (H) Heat map analysis showing relative mRNA expression profile of MK lineage–specific and related genes in UV-irradiated CVB3 (CVB3 UV) and CVB3 groups at 9 days after infection. The numbers in the heat map indicate the mean value of at least 4 independent samples. $^{\#}P < .05$ vs CVB3 UV using 1-way analysis of variance, $^{*}P < .05$ vs CVB3 UV using paired *t*-test, $^{\&}P < .05$ vs CVB3 UV on day 9 using 2-way analysis of variance, n = 3-6. CT, cycle threshold; DD, delta delta; *EEF1A1*, eukaryotic translation elongation factor 1 alpha 1; NS, not significant; VWF, von Willebrand factor.

determined using a concentration-response curve (Supplementary Figure S6).

In contrast, preincubation of $CD34^+$ cells with CU-CPT9, a highly selective TLR8 inhibitor, did not modify CVB3-mediated inhibition of megakaryopoiesis (Figure 6A–E), and stimulation with 2 TLR8-specific agonists (TL8-506 and ssPolyU) had no effect on either cell apoptosis or MK or platelet formation, even when used at high concentrations (Figure 6F–J). The activity of the TLR8 agonist and its inhibitor was confirmed by measuring the increase in IL-1β release in the supernatants of monocytes stimulated with TL8-506 in the absence or presence of the inhibitor (112 ± 2.9 pg/mL vs 67 ± 1.9 pg/mL; n = 2). Unexpectedly, the amounts of IL-1β elicited in CVB3-infected cultures were similar regardless of whether TLR7 was inhibited with ODN20958 or not (13 ± 2.8 pg/mL vs 14 ± 1.2 pg/mL; n = 4).

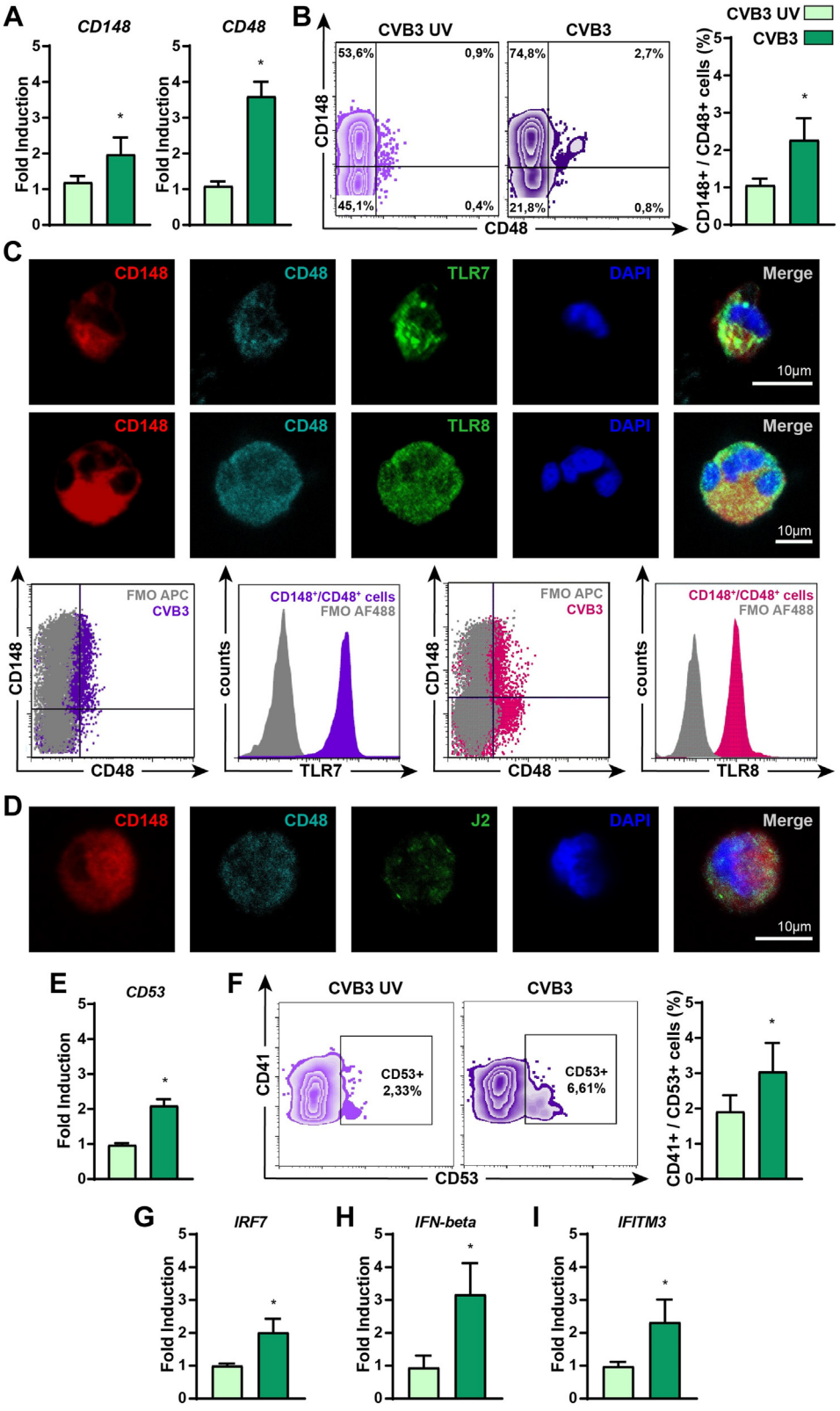

FIGURE 5 Coxsackievirus B3 (CVB3) of CD34$^+$ cells triggers the expansion of phenotypically immune megakaryocytes (MKs). CD34$^+$ cells were exposed to UV-irradiated CVB3 or CVB3 (multiplicity of infection, 1). (A) The mRNA expression levels of *CD148* and *CD48* were evaluated at 11 days after infection using quantitative polymerase chain reaction (qPCR). (B) CD148-PE/CD48-APC staining in the viable CD42b$^+$ MK subpopulation was determined at 12 days after infection. Representative zebra plots of 4 independent experiments and bar graph quantifying the percentages of CD148$^+$/CD48$^+$ cells. (C) Representative images and histograms of the expression of toll-like receptor 7 or 8 on immune MKs (CD148$^+$/CD48$^+$). (D) Representative microscopy images showing the expression of CD148 (red) and CD48 (cyan), J2 staining of double-

4 | DISCUSSION

Decreased platelet production causing thrombocytopenia has been observed in many viral infections [10,11]. During infection, host immune and nonimmune cells recognize virus-associated molecules via PRRs, such as TLRs and inflammasomes, and initiate an antiviral and inflammatory response by producing increased type I IFN and proinflammatory cytokines [37].

In this study, we described for the first time that TLR7 and TLR8 are expressed at the protein level in the megakaryocytic lineage and that the activation of TLR7 but not TLR8 with a ssRNA virus or synthetic agonists affects not only MK production but also platelet formation. Moreover, we also showed that viral infection and TLR7 activation trigger the appearance of a subset of immune inflammatory MKs.

TLR7 expression and functionality have been previously reported in $CD34^+$ cells from the bone marrow and platelets [38–40]. However, its expression and role during human megakaryo/thrombopoiesis remained unknown. In this study, we showed that TLR7 and TLR8 are both expressed in not only $CD34^+$ human cord blood–derived stem cells but also MK progenitors ($CD41^+/CD42b^-$ cells) and mature MKs ($CD41^+/CD42b^+$ cells). Moreover, these 3 types of megakaryocytic populations were susceptible to infection by CVB3, a ssRNA virus that is mainly recognized by TLR7 and TLR8 [41].

The CVB3 infection of $CD34^+$ cells resulted in fewer MKs that were associated with both apoptosis and pyroptosis. Remarkably, cell death was detected only in the last stages of MK development. This effect was not related to the differentiation process toward MKs because similar results were obtained when $CD34^+$ cells were expanded with stem cell factor and IL-3 without TPO (data not shown). Recently, extensive crosstalk among pyroptosis, apoptosis, and/or necroptosis was identified, leading to the emergence of the PANoptosis concept. The occurrence of PANoptosis has been described in some viruses [42]. Although we did not evaluate whether CVB3 also induces necroptosis, our findings suggest that viral recognition by $CD34^+$ cells and/or megakaryocytic cells triggers >1 cell death program that may contribute to the regulation of viral spread.

The CVB3 infection of $CD34^+$ cells not only decreased the formation of MKs but also significantly impaired MK maturation and differentiation as well as platelet formation. Interestingly, these effects were also observed when $CD34^+$ cells were infected with YFV (another ssRNA virus that induces thrombocytopenia [43]), suggesting that this is a more general response to ssRNA virus infection. The development of MKs involves the expression of molecules such as CD42b, CD42a, and VWF as well as an endomitotic process for expansion of the cytoplasm and formation of platelets [44]. Our results showed that CVB3 inhibits the expression of maturation markers by reducing the level of mRNA transcripts involved in MK maturation as well as lineage-specific transcription factors and regulators of thrombopoiesis, such as *NF-E2*. These findings strongly suggest that the thrombocytopenia observed in ssRNA viral infections may be due, in part, to substantial impairment of biological processes, leading to MK maturation and platelet production.

Previous studies have demonstrated that MK infection with another ssRNA, such as HIV-1 or Dengue virus, impairs MK survival and differentiation, leading to thrombocytopenia [45,46]. However, the role of endosomal TLR7/8 was not investigated in these studies. We found that both apoptosis and inhibition of MK as well as platelet formation by CVB3 or YFV infection of $CD34^+$ cells in the presence of specific TLR7 antagonists were not only completely abolished but also mimicked by synthetic TLR7 agonists such as loxoribine and imiquimod. Neither the inhibition of TLR8 nor the stimulation of $CD34^+$ cells with TLR8 agonists was able to alter the different stages of megakaryo/thrombopoiesis, suggesting a central role of TLR7 activation in the regulation of MK and platelet formation. These results are consistent with studies in nucleotide-binding oligomerization domain–containing (NOD) mice that showed that downregulation/upregulation of the TLR7 pathway by treating animals with CA-4948 or resiquimod, respectively, resulted in a consistent elevation/reduction of platelet counts that was associated with an increase in MK counts in the bone marrow with more naked nuclei in the resiquimod group [22].

Interestingly, we have previously described that Junin virus or TLR3 agonists induce thrombocytopenia without affecting megakaryopoiesis, suggesting that activation of endosomal TLR3 on $CD34^+$ progenitor cells impedes the process of thrombopoiesis rather than the generation of MKs [13,23]. These data and our current observations suggest that activation of each endosomal TLR regulates megakaryopoiesis and thrombopoiesis in different ways. In this regard, TLR3 agonists and Junin virus impair thrombopoiesis through IFN-β release [13,23]. In contrast, TLR7 activation by CVB3 resulted in only a modest increase in *IFN-β* mRNA expression, without detectable release of protein and without IFN-β–neutralizing Abs preventing the inhibition of megakaryo/thrombopoiesis. TLR3, which recognizes dsRNA, an intermediate for ssRNA viral replication, and TLR7 have different adaptor proteins after ligand binding in the endosomal compartment; although TLR3 uses the adaptor molecule TRIF, TLR7 signal transduction is dependent on the MyD88 adaptor protein [1]. More experiments are needed to determine whether the different responses in megakaryo/thrombopoiesis involve selective signaling molecules generated by the activation of these endosomal TLRs.

Besides TLRs, other different receptors, such as NOD-like receptors, have been described to sense RNA virus invasion, which regulates innate immunity by forming large molecular complexes (inflammasomes) that lead to caspase-1 activation and caspase-1–dependent proteolytic maturation and secretion of IL-1β

stranded RNA (green), and cell nuclei (blue). Scale bar, 10 μm. (E) The mRNA expression level of *CD53* was determined at 11 days after infection using qPCR. (F) $CD53^+$ MKs (gated on viable $CD41^+$ cells) at 12 days after infection. (G) The mRNA expression levels of *interferon regulatory factor 7*, (H) *interferon-β*, and (I) *interferon-induced transmembrane protein 3* were evaluated 24 hours after infection using qPCR, referred to as fold induction. $^*P < .05$ vs UV-irradiated CVB3 using paired *t*-test. qPCR data are referred to as fold induction, and *EEF1A1* was used as the housekeeping gene. DAPI, 4′,6-diamidino-2-phenylindole.

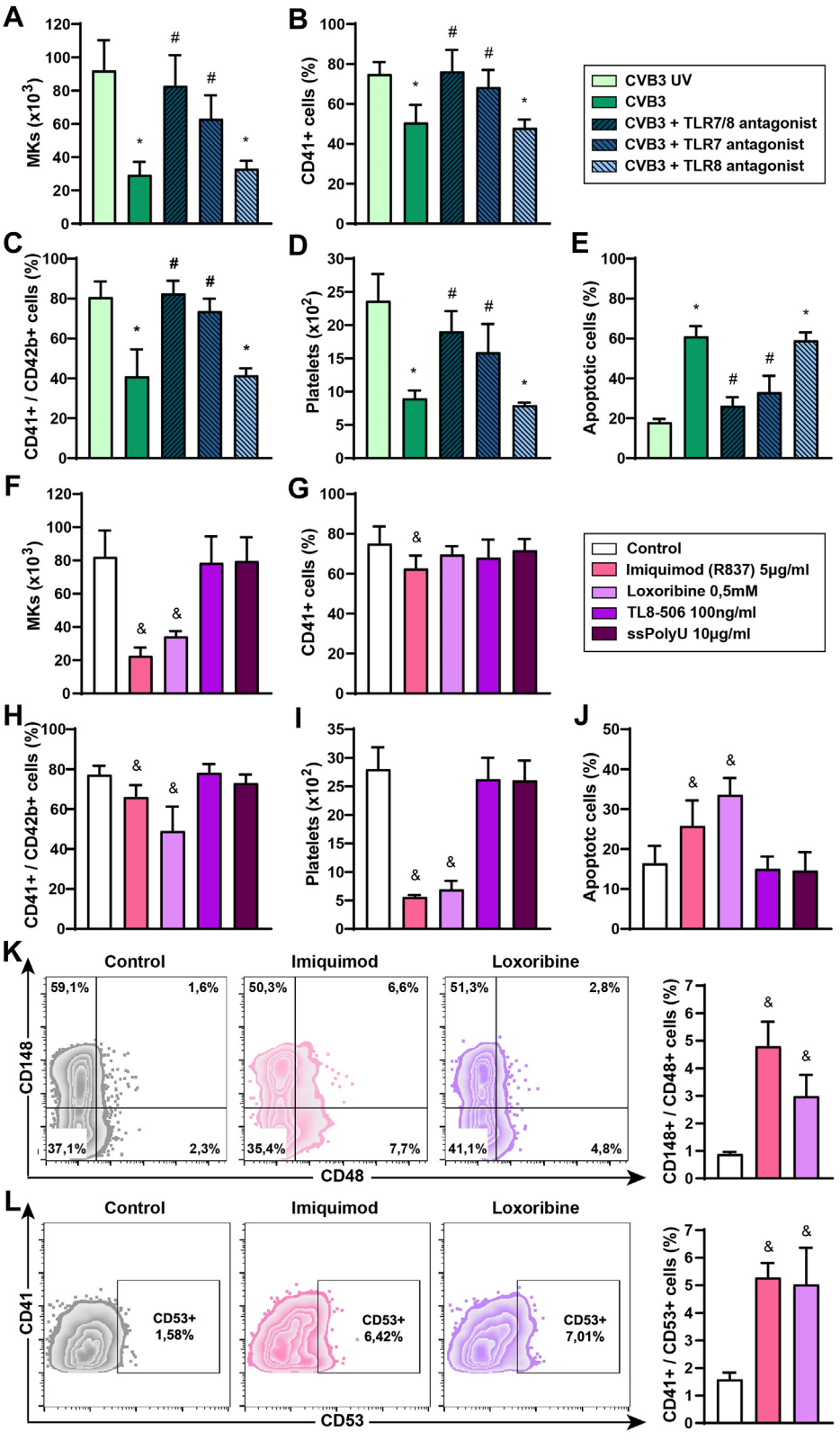

FIGURE 6 Toll-like receptor (TLR)7 mediates coxsackievirus B3 (CVB3) recognition, megakaryo/thrombopoiesis inhibition, and induction of a subpopulation of immune megakaryocytes (MKs). (A) The number of MKs, (B) percentage of $CD41^+$ cells and (C) $CD41^+/C42b^+$ cells, (D) number of platelets, and (E) percentage of apoptotic cells were determined in cultures of thrombopoietin (TPO)-stimulated $CD34^+$ cells that were pretreated or not with ODN2087 (TLR7/8 antagonist, 5 μM) or ODN20958 (TLR7 antagonist, 5 μM) for 1 hour or CU-CPT9a (TLR8 antagonist, 10 μM) for 3 hours and then exposed to UV-irradiated CVB3 or CVB3 (multiplicity of infection, 1). (F–J) $CD34^+$ cells were stimulated with TPO alone (control) or in combination with the TLR7 agonists loxoribine (0.5 mM) or imiquimod (R837, 5 μg/mL) or with the TLR8 agonists TL8-506 (100 ng/mL) or ssPolyU (10 μg/mL), and the same parameters as above were evaluated in these conditions. The number of MKs and platelets and the percentage of apoptotic cells were determined as described in Figure 2. (K) $CD34^+$ cells were treated with TLR7 agonists or not in the presence of TPO and CD148-PE/CD48-APC (gated on viable $CD42b^+$ cells), or (L) CD41-PE/CD53-FITC staining in the viable MK subpopulation was determined at 12 days after stimulation using flow cytometry. Representative zebra plots of 4 independent experiments. Bar graph quantifying the percentage of $CD148^+/CD48^+$ or $CD41^+/CD53^+$ cells (right to each panel). $^*P < .05$ vs UV-irradiated CVB3, $^{\#}P < .05$ vs CVB3 and $^{\&}P < .05$ vs control using 1-way analysis of variance, n = 4-6.

[47]. The involvement of NLRP3 inflammasomes during CVB3 infection and their relevance in CVB3-induced viral myocarditis have been demonstrated both *in vitro* and *in vivo* [48]. Our results showing the activation of inflammasome components at the RNA and protein levels in response to CVB3 infection are consistent with these findings. Surprisingly, the blockade of TLR7 did not alter CVB3-induced inflammasome activation and IL-1β release. In addition to TLR7, NOD-2 and the cytosolic helicases RIG-1 and MDA-5 have also been described as major PRRs that lead to NLRP3 activation in CVB3-induced myocarditis [49]. Moreover, protease $3C^{pro}$ from CVB3 is able to activate NLRP1 inflammasomes and induce IL-1β release [50]. Therefore, it would be conceivable that CVB3 activates not only TLR7 but also NOD-2, cytosolic helicases, or NLRP1.

Currently, it is believed that the population of MKs in mouse and human bone marrow is not homogeneous; however, there are specialized subsets of MKs that control platelet generation, interaction with the hematopoietic stem cell niche, and inflammatory/immune responses. Immune MKs in the bone marrow have been described as cells that are double positive for $CD148^+/CD48^+$ antigens and as low ploidy cells expressing CD53 and CD48. These cells appear to play an important role in inflammation/infections because their numbers increase upon stimulation with immune stimuli, such as LPS or IFN-γ, *in vitro* and *in vivo* [32,33]. We have now confirmed these findings and shown that mature MKs ($CD41^+/CD42b^+$) derived from cord blood also express CD148. In contrast to bone marrow MKs described by Liu et al. [32], we were unable to detect CD48 in these cells. However, MKs expressing mRNA and surface CD148/CD48 were generated in CVB3-infected cultures. In addition, we found a small percentage of $CD53^+$ MKs that significantly increased in virus-infected cells. Taken together, our data suggest that viral infection of HSPCs with CVB3 in the presence of TPO inhibits MK differentiation, maturation, and platelet production but increases the formation of immune MKs. In support of this hypothesis, a previous study showed that administration of LPS leads to a gradual increase in immune MKs, whereas the number of platelets in the periphery decreases [33]. Moreover, our results suggest that these MKs with an immune phenotype can arise from not only bacterial infection but also viral infection. Furthermore, we showed that immune MKs can be generated after $CD34^+$ stimulation and in response to TLR7 agonists, emphasizing a potential pivotal role of this receptor in the antiviral response of cells from the megakaryocytic lineage to infection with ssRNA. Patients with severe SARS-CoV-2 infection present with thrombotic coagulopathy associated with an increase in extramedullary MKs, especially in the lungs and heart, and IFN-activated MKs [51,52]. Interestingly, it is increasingly recognized that MKs from the lungs have stronger immunologic/inflammatory gene expression than bone marrow–derived MKs [53]. Whether the increased number of MKs observed in patients with COVID-19 includes these subpopulations of $CD148^+/CD48^+$ or $CD53^+$ immune MKs or whether these immune MKs produce more thromboinflammatory platelets is a very interesting area of research to investigate. Interestingly, in this context, the TLR7 activation of platelets by influenza and encephalomyocarditis viruses (ssRNA viruses) leads to P-selectin exposure and platelet-neutrophil interactions that are independent of platelet aggregation and contributes to immune response and host survival [20,39]. Whether these platelets are produced by immune MKs is a very challenging question that remains to be investigated.

In conclusion, we described here for the first time that TLR7 and TLR8 are expressed in HSPCs and MKs and that the activation of TLR7 in this lineage appears to be responsible for decreased platelet production due to cell death and inhibition of MK maturation, suggesting an additional mechanism involved in the decrease in platelet count during ssRNA viral infections. Our data also contribute to the new concept of MKs as cells with immune and inflammatory functions by describing a population of immune MKs resulting from TLR7 activation. Future studies on human cells using genetic approaches will hopefully confirm these findings. Understanding how MKs respond to infectious/inflammatory signals is critical for developing potential therapeutic options for clinical conditions associated with thrombocytopenia and/or thromboinflammation. Finally, we showed the adverse effects of synthetic TLR7 agonists that should be considered when these drugs are or could be used in clinical treatments or as adjuvant molecules.

FUNDING

This work was supported by grants from Agencia Nacional de Promoción Científica y Tecnológica (ANPCyT 2017-1188 and 2019-02307) and Grupo Cooperativo Argentino de Hemostasia y Trombosis (CAHTalizar 2021).

ETHICS STATEMENT

This study was conducted according to the principles expressed in the Declaration of Helsinki, and it was approved by the institutional review board of the National Academy of Medicine, Argentina (37/21/CEIANM). All individuals provided written informed consent for the collection of samples and subsequent analysis.

AUTHOR CONTRIBUTIONS

C.S.R. performed experiments, interpreted results, and wrote the manuscript. N.L.C. performed experiments. S.T. analyzed data and revised the manuscript. R.M.G. contributed to the design and analysis of the study. L.P.D. and M.S. designed the study, interpreted results, formulated discussion, wrote the manuscript, and assisted with manuscript preparation and editing. All the authors contributed to the analysis and/or interpretation of data and revision of intellectual content of the manuscript. All the authors gave their approval to the final version of the manuscript.

RELATIONSHIP DISCLOSURE

C.S.R. holds a fellowship from ANPCyT. N.L.C., R.M.G., L.P.D. and M.S. are scientific researchers from CONICET.

TWITTER

Camila Sofía Rodríguez @CamiSRodriguez @imex_conicetanm

REFERENCES

[1] Fitzgerald KA, Kagan JC. Toll-like receptors and the control of immunity. *Cell*. 2020;180:1044–66.

[2] Ebermeyer T, Cognasse F, Berthelot P, Mismetti P, Garraud O, Hamzeh-cognasse H. Platelet innate immune receptors and TLRs: a double-edged sword. *Int J Mol Sci*. 2021;22:7894.

[3] Hottz ED, Bozza FA, Bozza PT. Platelets in immune response to virus and immunopathology of viral infections. *Front Med*. 2018;5:121.

[4] D'Atri LP, Schattner M. Platelet Toll-like receptors in thromboinflammation. *Front Biosci*. 2017;22:1867–83.

[5] Maratheftis CI, Andreakos E, Moutsopoulos HM, Voulgarelis M. Toll-like receptor-4 is up-regulated in hematopoietic progenitor cells and contributes to increased apoptosis in myelodysplastic syndromes. *Clin Cancer Res*. 2007;13:1154–60.

[6] Zeng Q, Shu J, Hu Q, Zhou SH, Qian YM, et al. Apoptosis in human myelodysplastic syndrome $CD34^+$ cells is modulated by the upregulation of TLRs and histone H4 acetylation via a β-arrestin 1 dependent mechanism. *Exp Cell Res*. 2016;340:22–31.

[7] Paracatu LC, Monlish DA, Greenberg ZJ, Fisher DAC, Walter MJ, Oh ST, et al. Toll-like receptor and cytokine expression throughout the bone marrow differs between patients with low- and high-risk myelodysplastic syndromes. *Exp Hematol*. 2022;110:47–59.

[8] D'Atri LP, Rodríguez CS, Miguel CP, Pozner RG, Wilczyñski JM, Negrotto S, et al. Activation of toll-like receptors 2 and 4 on $CD34^+$ cells increases human megakaryo/thrombopoiesis induced by thrombopoietin. *J Thromb Haemost*. 2019;12:2196–210.

[9] Nilofar T, Sadique S, Natarajan T, Shanmugham K. Incidence of reactive thrombocytosis in serious bacterial infections in children aged two months to twelve years and its usefulness as a predictor of serious bacterial infections. *Int J Contemp Pediatr*. 2020;7:626–30.

[10] Schrottmaier WC, Schmuckenschlager A, Pirabe A, Assinger A. Platelets in viral infections—brave soldiers or Trojan horses. *Front Immunol*. 2022;13:856713.

[11] Raadsen M, du Toit J, Langerak T, van Bussel B, van Gorp E, Goeijenbier M. Thrombocytopenia in virus infections. *J Clin Med*. 2021;10:877.

[12] Pate KAM, Lyons CE, Dorsey JL, Queen SE, Adams RJ, Morrell CN, et al. TGFβ-mediated downregulation of thrombopoietin is associated with platelet decline in asymptomatic SIV infection. *J Acquir Immune Defic Syndr*. 2014;65:510–6.

[13] D'Atri LP, Etulain J, Rivadeneyra L, Lapponi MJ, Centurion M, Cheng K, et al. Expression and functionality of Toll-like receptor 3 in the megakaryocytic lineage. *J Thromb Haemost*. 2015;13:839–50.

[14] Getawa S, Aynalem M, Bayleyegn B, Adane T. The global prevalence of thrombocytopenia among HIV-infected adults: a systematic review and meta-analysis. *Int J Infect Dis*. 2021;105:495–504.

[15] Kaga A, Katata Y, Suzuki A, Otani K, Watanabe H, Kitaoka S, et al. Perinatal coxsackievirus B3 infection with transient thrombocytopenia. *Tohoku J Exp Med*. 2016;239:135–8.

[16] Negrotto S, De Giusti CJ, Rivadeneyra L, Ure AE, Mena HA, Schattner M, et al. Platelets interact with coxsackieviruses B and have a critical role in the pathogenesis of virus-induced myocarditis. *J Thromb Haemost*. 2015;13:271–82.

[17] Jansen AJG, Spaan T, Low HZ, Di Iorio D, Van Den Brand J, Tieke M, et al. Influenza-induced thrombocytopenia is dependent on the subtype and sialoglycan receptor and increases with virus pathogenicity. *Blood Adv*. 2020;4:2967–78.

[18] Yang X, Yang Q, Wang Y, Wu Y, Xu J, Yu Y, et al. Thrombocytopenia and its association with mortality in patients with COVID-19. *J Thromb Haemost*. 2020;18:1469–72.

[19] Liu Y, Sun W, Guo Y, Chen L, Zhang L, Zhao S, et al. Association between platelet parameters and mortality in coronavirus disease 2019: retrospective cohort study. *Platelets*. 2020;31:490–6.

[20] Koupenova M, Corkrey HA, Vitseva O, Manni G, Pang CJ, Clancy L, et al. The role of platelets in mediating a response to human influenza infection. *Nat Commun*. 2019;10:1780.

[21] Koupenova M, Corkrey HA, Vitseva O, Tanriverdi K, Somasundaran M, Liu P, et al. SARS-CoV-2 initiates programmed cell death in platelets. *Circ Res*. 2021;129:631–46.

[22] Zhang S, Qu J, Wang L, Li M, Xu D, Zhao Y, et al. Activation of Toll-like receptor 7 signaling pathway in primary Sjögren's syndrome-associated thrombocytopenia. *Front Immunol*. 2021;12:637659.

[23] Pozner RG, Ure AE, de Giusti CJ, D'Atri LP, Italiano JE, Torres O, et al. Junín virus infection of human hematopoietic progenitors impairs in vitro proplatelet formation and platelet release via a bystander effect involving type I IFN signaling. *PLoS Pathog*. 2010;6:e1000847.

[24] Robert A, Cortin V, Garnier A, Pineault N. Megakaryocyte and platelet production from human cord blood stem cells. *Methods Mol Biol*. 2012;788:219–47.

[25] Renvoizé C, Biola A, Pallardy M, Bréard J. Apoptosis: identification of dying cells. *Cell Biol Toxicol*. 1998;14:111–20.

[26] Hayashi F, Means TK, Luster AD. Toll-like receptors stimulate human neutrophil function. *Blood*. 2003;102:2660–9.

[27] Rivadeneyra L, Charó N, Kviatcovsky D, de la Barrera S, Gómez RM, Schattner M. Role of neutrophils in CVB3 infection and viral myocarditis. *J Mol Cell Cardiol*. 2018;125:149–61.

[28] Bergelson JM, Cunningham JA, Droguett G, Kurt-Jones EA, Krithivas A, Hong JS, et al. Isolation of a common receptor for coxsackie B viruses and adenoviruses 2 and 5. *Science*. 1997;275:1320–3.

[29] de Vasconcelos NM, Van Opdenbosch N, Van Gorp H, Parthoens E, Lamkanfi M. Single-cell analysis of pyroptosis dynamics reveals conserved GSDMD-mediated subcellular events that precede plasma membrane rupture. *Cell Death Differ*. 2018;26:146–61.

[30] Michelson AD, Ellis PA, Barnard MR, Matic GB, Viles AF, Kestin AS. Downregulation of the platelet surface glycoprotein Ib-IX complex in whole blood stimulated by thrombin, adenosine diphosphate, or an in vivo wound. *Blood*. 1991;77:770–9.

[31] Montague SJ, Andrews RK, Gardiner EE. Mechanisms of receptor shedding in platelets. *Blood*. 2018;132:2535–45.

[32] Liu C, Wu D, Xia M, Li M, Sun Z, Shen B, et al. Characterization of cellular heterogeneity and an immune subpopulation of human megakaryocytes. *Adv Sci*. 2021;8:2100921.

[33] Sun S, Jin C, Si J, Lei Y, Chen K, Cui Y, et al. Single-cell analysis of ploidy and the transcriptome reveals functional and spatial divergency in murine megakaryopoiesis. *Blood*. 2021;138:1211–24.

[34] Negrotto S, De Giusti CJ, Lapponi MJ, Etulain J, Rivadeneyra L, Pozner RG, et al. Expression and functionality of type I interferon receptor in the megakaryocytic lineage. *J Thromb Haemost*. 2011;9:2477–85.

[35] Campbell RA, Schwertz H, Hottz ED, Rowley JW, Manne BK, Washington AV, et al. Human megakaryocytes possess intrinsic antiviral immunity through regulated induction of IFITM3. *Blood*. 2019;133:2013–26.

[36] Heil F, Ahmad-Nejad P, Hemmi H, Hochrein H, Ampenberger F, Gellert T, et al. The Toll-like receptor 7 (TLR7)-specific stimulus loxoribine uncovers a strong relationship within the TLR7, 8 and 9 subfamily. *Eur J Immunol*. 2003;33:2987–97.

[37] Carty M, Guy C, Bowie AG. Detection of viral infections by innate immunity. *Biochem Pharmacol*. 2020;183:114316.

[38] Sioud M, Fløisand Y, Forfang L, Lund-Johansen F. Signaling through Toll-like receptor 7/8 induces the differentiation of human bone marrow $CD34^+$ progenitor cells along the myeloid lineage. *J Mol Biol*. 2006;364:945–54.

[39] Koupenova M, Vitseva O, MacKay CR, Beaulieu LM, Benjamin EJ, Mick E, et al. Platelet-TLR7 mediates host survival and platelet count

during viral infection in the absence of platelet-dependent thrombosis. *Blood*. 2014;124:791–802.

[40] Koupenova M, Mick E, Mikhalev E, Benjamin EJ, Tanriverdi K, Freedman JE. Sex differences in platelet toll-like receptors and their association with cardiovascular risk factors significance. *Arterioscler Thromb Vasc Biol*. 2015;35:1030–7.

[41] Triantafilou K, Orthopoulos G, Vakakis E, Ahmed MAE, Golenbock DT, Lepper PM, et al. Human cardiac inflammatory responses triggered by coxsackie B viruses are mainly Toll-like receptor (TLR) 8-dependent. *Cell Microbiol*. 2005;7:1117–26.

[42] Nguyen LN, Kanneganti TD. PANoptosis in viral infection: the missing puzzle piece in the cell death field. *J Mol Biol*. 2022;434:167249.

[43] Ho YL, Joelsons D, Leite GFC, Malbouisson LMS, Song ATW, Perondi B, et al. Severe yellow fever in Brazil: clinical characteristics and management. *J Travel Med*. 2019;26:taz040.

[44] Noetzli LJ, French SL, Machlus KR. New insights into the differentiation of megakaryocytes from hematopoietic progenitors. *Arterioscler Thromb Vasc Biol*. 2019;39:1288–300.

[45] Costantini A, Giuliodoro S, Mancini S, Butini L, Regnery CM, Silvestri G, et al. Impaired in-vitro growth of megakaryocytic colonies derived from CD34 cells of HIV-1-infected patients with active viral replication. *AIDS*. 2006;20:1713–20.

[46] Basu A, Jain P, Gangodkar SV, Shetty S, Ghosh K. Dengue 2 virus inhibits in vitro megakaryocytic colony formation and induces apoptosis in thrombopoietin-inducible megakaryocytic differentiation from cord blood $CD34^+$ cells. *FEMS Immunol Med Microbiol*. 2008;53:46–51.

[47] Shrivastava G, León-Juárez M, García-Cordero J, Meza-Sánchez DE, Cedillo-Barrón L. Inflammasomes and its importance in viral infections. *Immunol Res*. 2016;64:1101–17.

[48] Wang Y, Gao B, Xiong S. Involvement of NLRP3 inflammasome in CVB3-induced viral myocarditis. *Am J Physiol Heart Circ Physiol*. 2014;307:H1438–47.

[49] Tschöpe C, Müller I, Xia Y, Savvatis K, Pappritz K, Pinkert S, et al. NOD2 (nucleotide-binding oligomerization domain 2) is a major pathogenic mediator of coxsackievirus B3-induced myocarditis. *Circ Hear Fail*. 2017;10:e003870.

[50] Tsu BV, Beierschmitt C, Ryan AP, Agarwal R, Mitchell PS, Daugherty MD. Diverse viral proteases activate the nlrp1 inflammasome. *Elife*. 2021;10:e60609.

[51] Bernardes JP, Mishra N, Tran F, Bahmer T, Best L, Blase JI, et al. Longitudinal multi-omics analyses identify responses of megakaryocytes, erythroid cells, and plasmablasts as hallmarks of severe COVID-19. *Immunity*. 2020;53:1296–314.

[52] Meyerholz DK, McCray PB. Illuminating COVID-19 lung disease through autopsy studies. *EBioMedicine*. 2020;57:102865.

[53] Pariser DN, Hilt ZT, Ture SK, Blick-Nitko SK, Looney MR, Cleary SJ, et al. Lung megakaryocytes are immune modulatory cells. *J Clin Invest*. 2021;131:e137377.

SUPPLEMENTARY MATERIAL

The online version contains supplementary material available at https://doi.org/10.1016/j.rpth.2023.100184